

# **ADVANCES IN FOREST FIRE RESEARCH**

**2022**

**Edited by**

**DOMINGOS XAVIER VIEGAS  
LUÍS MÁRIO RIBEIRO**

## Fire-spotting modelling: A comparative study of an Italian test case

Marcos López-De-Castro\*<sup>1</sup>; Andrea Trucchia<sup>2</sup>; Umberto Morra di Cella<sup>2</sup>; Paolo Fiorucci<sup>2</sup>,  
Antonio Cardillo<sup>3</sup>, Gianni Pagnini<sup>1,4</sup>

<sup>1</sup> *BCAM-Basque Center for Applied Mathematics. Calle Alameda de Mazarredo 14,  
Bilbao, 48009, Basque Country, Spain,  
{malopez, gpagnini}@bcamath.org*

<sup>2</sup> *CIMA Research Foundation. Via Armando Magliotto 2, Savona, 17100, Italy, {andrea.trucchia,  
paolo.fiorucci, umberto.morradicella}@cimafoundation.org*

<sup>3</sup> *Regione Molise, Centro Funzionale Decentrato del Molise,  
Contrada Selva del Campo, Campochiaro, 86020, Italy,  
{cardillo@protezionecivile.molise.it}*

<sup>4</sup> *Ikerbasque-Basque Foundation for Science. Plaza Euskadi 5,  
Bilbao, 48009, Basque Country, Spain.*

*\*Corresponding author*

### Keywords

Wildfire simulation, fire-spotting, RandomFront, PROPAGATOR, cellular automata.

### Abstract

Wildfire propagation is a non-linear and multiscale system in which there are involved multiple physical and chemical processes. One critical mechanism for the spreading of wildfires is the so-called fire-spotting: a random phenomenon which occurs when embers are transported over large distances by the wind, and causing the start of new spotting ignitions which jeopardize the fire-fighting actions. Due to its nature, fire-spotting is usually modeled as a probabilistic process. Three principal processes are involved during the fire-spotting: firebrands generation, transport joined with landing, and spot ignition. In this work, the physical parametrization of fire-spotting RandomFront (Trucchia et al. 2019) has been implemented into the operational wildfire spread simulator PROPAGATOR (Trucchia et al. 2020), which is based on a cellular automata approach. In the routine RandomFront, the downwind landing distribution of firebrands is modeled by means of a lognormal distribution, which is parameterized by taking into account the physics involved in the phenomenon. The considered physical parameters are: wind field, fire-line intensity, fuel density, firebrand radius, maximum loftable height, as well as factors related to atmospheric stability and flame geometry (Trucchia et al. 2019; Egorova et al. 2020,2022). As a matter of fact, similarity analysis cannot be applied to wildfires (Egorova et al. 2022, Section 2) thus the outputs of the simulations are checked against a real test case. In particular, we have considered the evolution of a real wildfire occurred in Italy in August 2021 during which the fire-spotting played a critical role. In addition, we have implemented into PROPAGATOR also other two schemes for fire-spotting already available in literature and suitable for cellular automata-based wildfire simulators (Alexandridis et al. 2011; Perryman et al. 2013). We compared the performance of these three fire-spotting models. The results show that, on the one hand, the RandomFront parametrization reproduces the main spotting effects similarly to the available literature models (Alexandridis et al. 2011; Perryman et al. 2013), and, on the other hand, RandomFront generates also a variety of fire-spotting situations together with long-range fluctuations of the burning probability by allowing for complex patterns.

### 1. Brief introduction

Fire-spotting occurs when firebrands are transported away from fire and start new fires known as spot-fires (Brown and Davis 1973; Werth et al. 2011). These new fires can occur near the fire propagation front, accelerating the spread of fire, or kilometers away from the source fire, causing new secondary ignitions that increase the extinction difficulty and in which civilians and firefighters can result trapped (Koo et al. 2010). The conducted research to understand this phenomenon has been done in two ways. On one hand, there are extensive experimental studies focused on the characterization of the firebrands generation and transport process (Manzello et al. 2007, 2008; Suzuki et al. 2012; Thomas et al. 2017; Himoto and Iwami 2021; Wickramasinghe et al. 2022). Unfortunately, the short scales of the experiments limit its application into the calculation of the landing distribution (Pérez et al. 2011; Sullivan and Cruz 2015). On the other hand, firebrand transport models

have been developed to estimate the landing distribution and flight paths of the firebrands (Tarifa et al. 1965, 1967; Albini 1979, 1983; Himoto and Tanaka 2005; Sardoy et al. 2007, 2008; Wang 2011; Kaur et al. 2016). We highlight that the validation of these models in reduce-scale experiments are unreliable, in particular, in cases with important wind-fire or multiple fire interactions (Egorova et al. 2022, Section 2).

Wildfire modeling has been studied from several approaches (Sullivan 2009a; b; c), but Cellular Automata (CA) based methods have demonstrated to be a quick, efficient, and versatile approach to simulate the wildfire spreading (Clarke et al. 1994, Duarte 1997, Hargrove et al. 2000, Encinas et al. 2007, Gharakhanlou and Hooshangi 2021). Some of the developed CA-based models include the effect of the fire-spotting. We highlight the model developed by Alexandridis et al. (2008, 2011), which was revisited by Freire and Dacamara (2019) to reproduce a forest fire in Portugal, and the model developed by Perryman et al. (2013).

In this work, we have implemented into the operational wildfire spread simulator PROPAGATOR (Trucchia et al. 2020) the recently developed parametrization RandomFront (Trucchia et al. 2019; Egorova et al. 2020, 2022) as well as both previously cited CA-based fire-spotting models to be compared. In addition, we have reproduced a wildfire that occurred in Italy in August 2021, in which the fire-spotting effects were critical, for validating the results.

## 2. Fire propagation model and firebrand landing parametrizations description

### 2.1. Propagator fire-spread simulator

In this work, PROPAGATOR (Trucchia *et al.* 2020) was used to simulate the spread of fire. PROPAGATOR is an operational software based on a CA approach and assisted with high resolution data from the topography and land fuel cover. The fire spread is computed through vegetation type, slope, wind direction and speed, and fuel moisture content, therefore, the burned surface evolves in a stochastic sense. The input parameters are the wind intensity and direction, the start point of fire and the adopted ROS model. PROPAGATOR is designed to compute an ensemble of simulations in a fast way, being its basic and natural output a georeferenced map which represents the probability of each cell to be affected by fire.

### 2.2. Alexandridis *et al.* (2011) firebrand landing parametrization

The model developed by Alexandridis et al. (2008, 2011), consist of a CA approach focused on the efficient simulation of wildfire spreading. The first part of their fire-spotting parametrization models the firebrand landing distance as follows:

$$d_p = r_n \cdot P_w = r_n \exp\left(U_{C_2}(\cos \varphi - 1)\right), \quad (1)$$

where  $r_n$  is a random number drawn from a normal distribution,  $\varphi$  is the angle between the direction of the wind and the direction of the blasting, and  $U_{C_2} = U \cdot C_2$  is the mean-wind velocity times a fitted constant. In addition, the probability of spot ignition, *i.e.*, when a blasting firebrand will ignite or not a new spot-fire, is computed as:

$$P_C = P_{C0} (1 + P_{cd}), \quad (2)$$

where  $P_{C0}$  is a constant probability corrected by  $P_{cd}$ , which is a factor that depends on type and fuel density.

### 2.3. Perryman *et al.* (2013) firebrand landing parametrization

The model developed by Perryman et al. (2013) consists of an ensemble of four sub-models adapted to a CA environment. Their firebrand landing distribution was implemented following the statistical model developed by Sardoy et al. (2008) for the firebrands which are blasted parallel to the wind, and the Himoto and Tanaka (2005) results for firebrands blasted perpendicular to the wind field. The landing distance of the parallel firebrands are computed following a lognormal distribution function:

$$p(d) = \frac{1}{(\sqrt{2\pi} \sigma_{FB} d)} \exp\left(\frac{-(\ln(d) - \mu_{FB})^2}{(2\sigma_{FB}^2)}\right), \quad (3)$$

where  $d$  is the distance away from the line front. The mean  $\mu_{FB}$  and standard deviation  $\sigma_{FB}$  depend on the current wind intensity  $U$ , the fireline intensity  $I_f$ , fitted constants and if the firebrands are buoyancy driven or wind driven. To discern between both cases, the Froude number  $Fr$  is computed:

$$Fr = \frac{U}{\sqrt{g \left( \frac{I_f}{(\rho c_p T_A g^{1/2})} \right)^{2/3}}}, \quad (4)$$

where  $g$  is the acceleration of gravity,  $I_f$  is the fire intensity,  $\rho$  is the ambient gas density,  $c_p$  is the specific heat of gas and  $T_A$  is the ambient temperature. If Froude number is less or equal to one, buoyancy driven regime is considered and for Froude number greater than one, wind driven plume regime. The firebrand distance of the embers generated parallel to the wind are modeled by means of a normal distribution, assuming zero mean and standard deviation  $\sigma_v = L/2$ , where  $L$  is the cell size.

#### 2.4. RandomFront firebrand landing parametrization

The landing distance is parameterized by means of a log-normal distribution (*i.e.*, Eq. (3)) combined with the physics involved in the firebrand transport (Trucchia *et al.* 2019). The mean of the distribution  $\mu^*$  depends strongly on the atmospheric conditions, specifically on the Atmospheric boundary layer (Egorova *et al.* 2020):

$$\mu^* = H \left( \frac{3\rho C_d}{2\rho_f} \right)^{1/2}, \quad (5)$$

where  $C_d$  is de Drag coefficient and  $\rho_f$  is the density of the wildland fuels. The maximum liftable height of the firebrands  $H$  is computed as a fraction of the injection height  $H = 0.4 \cdot H_{smoke}$ . The injection height of the smoke  $H_{smoke}$  is described by the formula (Sofiev *et al.* 2012, formula (10)):

$$H_{smoke} = \alpha H_{ABL} + \beta \left( \frac{I_f}{d P_{f0}} \right)^\zeta \exp \left( - \frac{\delta_{FT} N_{FT}^2}{N_0^2} \right), \quad (6)$$

where  $H_{ABL}$  is the height of the atmospheric boundary layer,  $N_0^2$  and  $N_{FT}^2$  are the Brunt-Väisälä frequency at the current height and in the free troposphere respectively, and  $P_{f0}$  is the ratio of reference fire power. The standard deviation  $\sigma$  involves the effects of the horizontal wind, flame geometry and the slope over the fire-spotting landing distance Egorova *et al.* (2020, 2022):

$$\sigma = \sigma(\varphi, \omega) = \frac{1}{z_p} \ln \left\{ \frac{U \cos \varphi}{\sqrt{gr(1 + \tan^2 \omega)}} + \beta_2 \sqrt{\frac{2\rho_f}{3\rho C_d}} \frac{1.4U \cos \varphi + \sqrt{gh_0(1 + \phi_{wind} + \phi_{slope})^{2/3}} \tan \omega}{\sqrt{gh_0(1 + \phi_{wind} + \phi_{slope})^{2/3}} - 1.4U \cos \varphi \tan \omega} \right\}, \quad (7)$$

where  $\varphi$  is the angle between the wind and the direction in which a firebrand is ejected,  $\omega$  is the slope of the cell in which the ember is generated and:

$$L_f = h_0 \left( 1 + \phi_{wind} + \phi_{slope} \right)^{2/3} = \beta_0 I_f^{2/3}, \quad (8)$$

where:

$$\beta_0 = \left( \frac{1}{2g(\rho c_p T_A)^2} \right)^{1/3}. \quad (9)$$

Fire-spotting in the RandomFront parametrization is considered as a downwind phenomenon. A critical angle  $\varphi_0$  is defined as the angle for which the ember is not considered ( $\sigma \leq 0$ ). By means of the probabilistic distribution, this is the angle for which  $\sigma$  becomes negative.

### 3. Area of study and simulations

#### 3.1. Area of study

The reproduced wildfire took place 1<sup>st</sup> August 2021 in the municipality of Campomarino, in the Adriatic coast of Italy (Fig. 1).

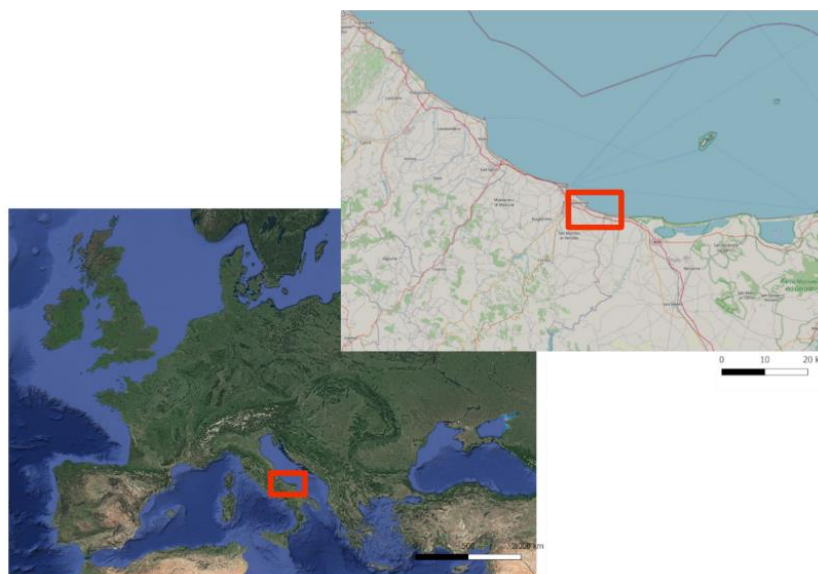


Figure 1- Study area.

The burnt perimeter is exposed in Fig. 2 – (a). The wildfire started burning around 12:00 am and finished around 5:00 pm. The fire-spotting effects were reported around 3:00 pm from the East to the West part of the port. We defined a rectangular area of study with 2.98 km<sup>2</sup> around the wildfire extension to run the simulations. Each cell of the cellular automaton has a resolution of 20 m<sup>2</sup>. The fuel types have been adapted from the Corine Land Cover (CLC) classification (Feranec et al. 2016) to the propagator classes (Fig. 2 – (b)). Specifically, we took *Pinus pinaster Aiton* as the reference tree specimen associated with the fire-prone conifers fuel type (Tihay et al. 2009). The data labeled as “non-burnable” have a low but non-zero probability of being burnt. The orography data were obtained from a Digital Elevation Model (DEM) but due to the proximity to the sea, a null or very tiny variation of the slope is reported over the fire-prone conifers.

#### 3.2. Methodology and simulations

For each parametrization an ensemble of 100 independent realizations was generated under the same conditions (Trucchia et al. 2020). The computational time for each ensemble is less than two minutes. Each simulation was stopped after 5 hours of simulated time. The weather was reported to be unstable and turbulent when the wildfire occurred, with peaks up to 70 km/h. To reproduce these conditions, we consider a constant wind speed of 40 km/h and, each 15 minutes of simulated time, a stochastic constant derived from a normal distribution with mean 0 and standard deviation 20 is added to the mean wind speed. In addition, the main wind direction, which came mainly from south, is also perturbed each 15 min with a stochastic variable derived from a normal distribution with mean 0 and standard deviation  $\pi/8$ . Two processes still needed to be characterized for a complete fire-spotting description: firebrand generation and spot ignition. Despite the considerable number of studies focused on both previous phenomena at the laboratory scale, there is a lack of research focused on the development of a physics-guided probabilistic model to characterize them. Due to this reason, we have modeled the firebrand generation for each burning cell by means of a Poisson distribution and the spot probability through Eq. (2). Next, we show the probability maps computed from the ensemble of simulations after 3 and 5 hours, which are the times at which fire-spotting was reported and the fire stopped, respectively.

##### 3.2.1. Alexandridis et. al. (2011) sub-model results

The port separates both coniferous areas with 190 m, so the mean of the normal distribution which will generate  $r_n$  in the Alexandridis parametrization Eq. (1) was implemented as 190. We also consider to implement the

standard deviation equal to 25 as reasonable value. The computed burn probability map for this firebrand landing distribution after 3 and 5 hours is exposed in Figure 3 respectively.

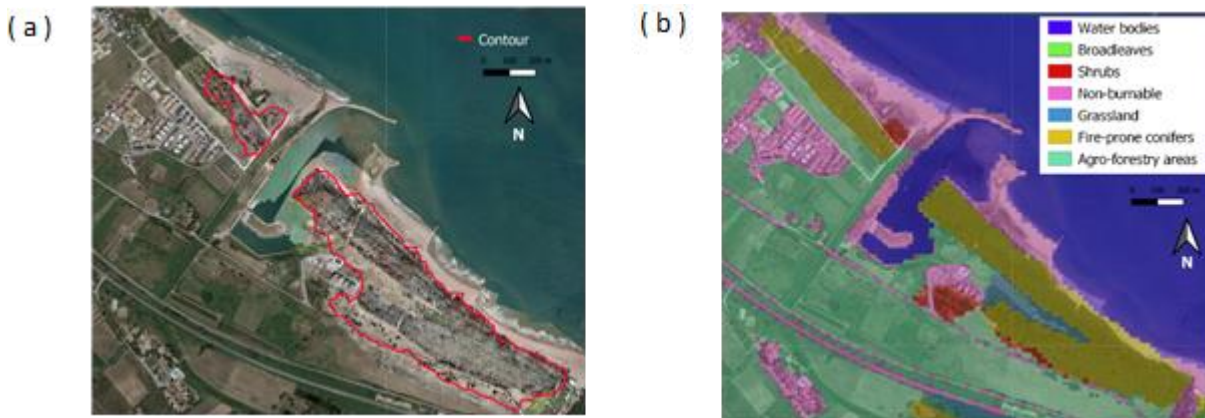


Figure 2- Studied area. Figure 2-(a) shows the true color orthomosaic derived by UAV survey done after the wildfire occurs. The red line defined the burnt area, based on high resolution photointerpretation. Figure 2-(b) displays the land cover classification used.

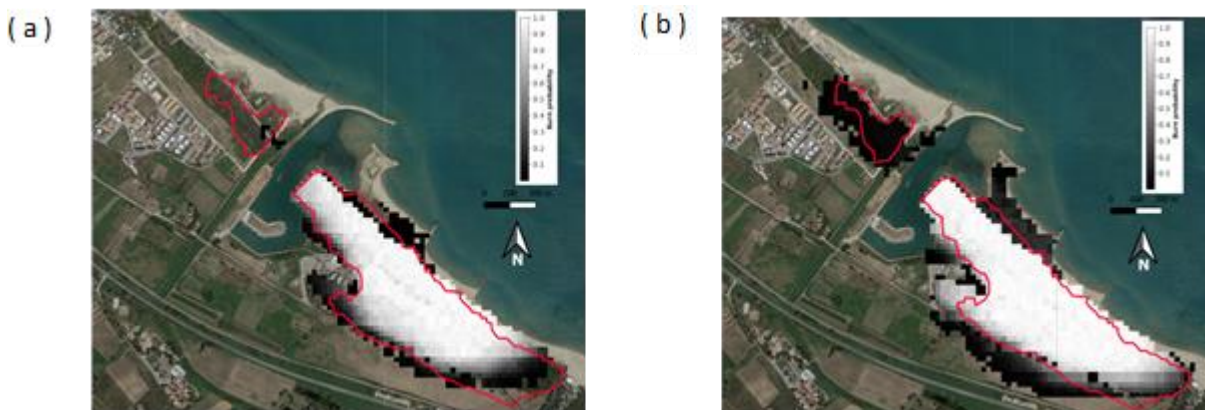


Figure 3- Computed burn probability map with the Alexandridis parametrization implemented. Figure 3-(a) shows the burn probability after 3 hours and Figure 3-(b) after 5 hours.

### 3.2.2. Perryman et. al. (2013) sub-model results

The burn probability map after 3 and 5 hours with the Perryman firebrand landing distribution is shown in Figure 4.

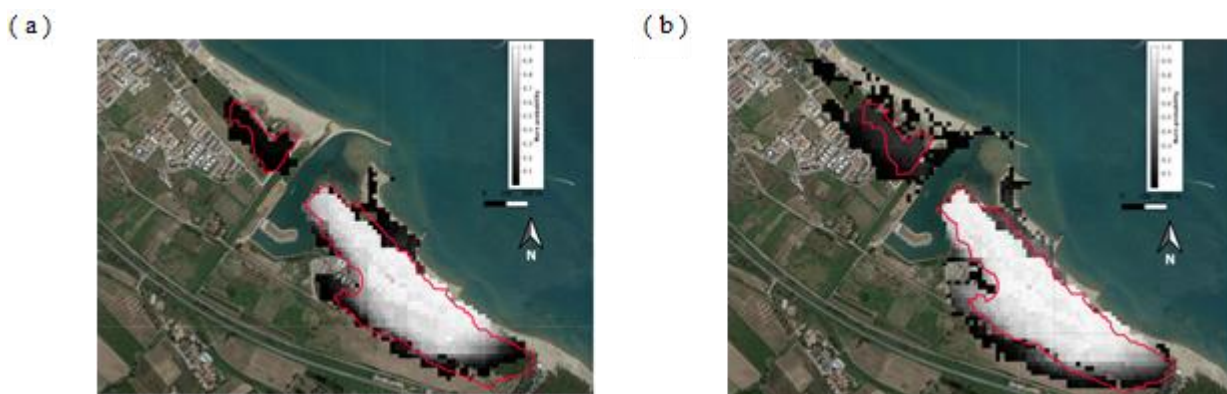


Figure 4- Computed burn probability map with the Perryman parametrization implemented. Figure 4-(a) shows the burn probability after 3 hours and Figure 4-(b) after 5 hours.

### 3.2.3. RandomFront sub-model results

The burn probability map after 3 and 5 hours with the RandomFront firebrand landing distribution is shown in Figure 5. Due to the instability of the weather and the summer conditions we consider the height of the Atmospheric Boundary Layer equal to  $H_{abl} = 2600$  m.

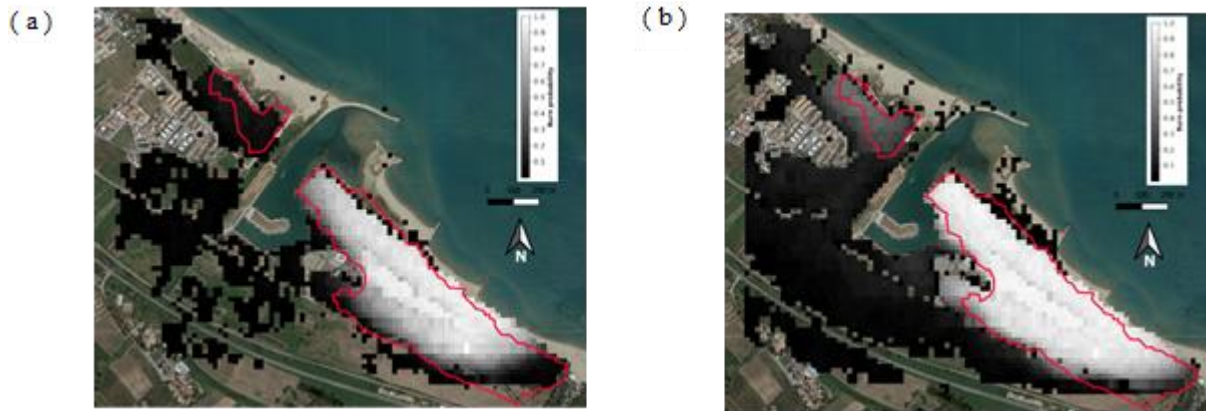


Figure 5- Computed burn probability map with the RandomFront parametrization implemented. Figure 5-(a) shows the burn probability after 3 hours and Figure 5-(b) after 5 hours

## 4. Brief discussion

To validate the model against the shape of the reference wildfire and quantify the obtained results, the averaged probability was computed for the two reference areas at both sides of the port, see Table 1. This measure is defined as the sum of the probabilities associated to each cell in the reference domains divided by the number of cells inside the reference domains.

Table 1- Averaged probabilities computed inside the reference perimeters.

Area	Alexandridis <i>et al.</i> (2011)	Perryman <i>et al.</i> (2013)	RandomFront
East	0.7937	0.7370	0.7303
West	0.0358	0.1330	0.2868

Table 1 shows that the averaged probability in the reference area at the West part of the port is, in the ensemble generated with RandomFront parametrization, one order of magnitude higher than the one obtained by using Alexandridis *et al.*, and more than twice when compared with the Perryman *et al.* parametrization. This agrees with Figures 3, 4 and 5 displayed results. Figure 3 shows how Alexandridis *et al.* parametrization is unable to assign any burning probability to the West part of the port when the fire-spotting was indeed reported. In addition, at the end of the simulation, a poor spread pattern is observed. The Perryman *et al.* parametrization of the firebrand's landing distribution displayed in Figure 4 generates a bit more complex spread pattern than by using Alexandridis *et al.*, but a low burn probability remains assigning to the West part of the port. By contrast, RandomFront firebrand's landing parametrization can generate a clear but low burn probability when the fire-spotting was reported. In addition, at the end of the simulation, an averaged burnt probability of 28.6% is assigned to the reference area at the West part of the port, as well as quite complex spread pattern is observed.

The implementation of fire-spotting routines causes deviation between simulations output when performed with different fire-spotting models (but fixed input data), see Figures 3, 4 and 5. In particular, from both the spread pattern and the probability to burn, we have that that the fire-spotting parametrization RandomFront performs better than the other two models.

## 5. Main conclusions

In this work, we have implemented the recently developed RandomFront fire-spotting landing distribution into the operational software PROPAGATOR. In addition, we have compared against other two fire-spotting models developed for a cellular automaton setting. To compare the performance of these three parametrizations, a real wildfire affected by fire-spotting effects was reproduced and used as validation test: actually, because results at laboratory scale are unreliable due to the multi-scale nature of wildfires. The ensemble computed with the

RandomFront parametrization displays a more complex spread pattern than the other parametrizations and a non-zero burnt probability in the West area of the port where the fire-spotting was indeed reported. In addition, at the end of the simulation in the area affected by the fire-spotting, RandomFront provides higher burnt probabilities than the other implemented parametrizations. Firebrand rate generation and spot ignition probability, which are still poorly for probabilistic modelling approaches, embody future development of the present research.

## **6. Acknowledgements:**

This research has been supported by the Basque Government through the BERC 2022–2025 programme; by the Spanish Ministry of Economy and Competitiveness (MINECO) through the BCAM Severo Ochoa excellence accreditation SEV-2017-0718 and also through the project PID2019-107685RB-I00; by the European Regional Development Fund (ERDF) and the Department of Education of the regional government, the Junta of Castilla y León (Grant 574 contract SA089P20); and by the Interreg IPA CBC Italy- Albania - Montenegro programme through the project The flood and Big fire foREst, prediction, forecAst and emergencY management (TO BE READY).

## **7. References:**

- Albini F (1979) Spot fire distance from burning trees -a predictive model. USDA Forest Service, Intermountain Forest and Range Experiment Station, General Technical Report INT-56. (Odgen, UT).
- Albini F (1983) Potential spotting distance from wind-driven surface fires. USDA Forest and Range Experiment Station, Research paper INT-309. (Odgen, UT).
- Alexandridis A, Russo L, Vakalis D, Bafas GV, Siettos CI (2011) Wildland fire spread modelling using cellular automata: evolution in large-scale spatially heterogeneous environments under fire suppression tactics. *International Journal of Wildland Fire* 20, 633. doi:10.1071/WF09119.
- Alexandridis A, Vakalis D, Siettos CI, Bafas GV (2008) A cellular automata model for forest fire spread prediction: The case of the wildfire that swept through Spetses Island in 1990. *Applied Mathematics and Computation* 204, 191–201. doi:10.1016/j.amc.2008.06.046.
- Brown AA, Davis KP (1973) ‘Forest fire: control and use.’ (McGraw-Hill: New York)
- Clarke K, Brass J, Riggan P (1994) A Cellular Automaton Model of Wildfire Propagation and Extinction. *Photogrammetric Engineering and Remote Sensing* 60(11), 1355–1367.
- Duarte JAMS (1997) Bushfire Automata and Their Phase Transitions. *International Journal of Modern Physics C* 08, 171–189. doi:10.1142/S0129183197000175.
- Egorova VN, Trucchia A, Pagnini G (2020) Fire-spotting generated fires. Part I: The role of atmospheric stability. *Applied Mathematical Modelling* 84, 590–609. doi:10.1016/j.apm.2019.02.010.
- Egorova VN, Trucchia A, Pagnini G (2022) Fire-spotting generated fires. Part II: The role of flame geometry and slope. *Applied Mathematical Modelling* 104, 1–20. doi:10.1016/j.apm.2021.11.010.
- Encinas LH, White SH, Rey AM del, Sánchez GR (2007) Modelling forest fire spread using hexagonal cellular automata. *Applied Mathematical Modelling* 31, 1213–1227. doi:https://doi.org/10.1016/j.apm.2006.04.001.
- Feranec J, Soukup T, Hazeu G, Jaffrain G (Eds) (2016) ‘European Landscape Dynamics.’ (CRC Press) doi:10.1201/9781315372860.
- Freire JG, DaCamara CC (2019) Using cellular automata to simulate wildfire propagation and to assist in fire management. *Natural Hazards and Earth System Sciences* 19, 169–179. doi:10.5194/nhess-19-169-2019.
- Gharakhanlou NM, Hooshangi N (2021) Dynamic simulation of fire propagation in forests and rangelands using a GIS-based cellular automata model. *International Journal of Wildland Fire* 30, 652–663. doi:10.1071/WF20098.
- Hargrove WW, Gardner RH, Turner MG, Romme WH, Despain DG (2000) Simulating fire patterns in heterogeneous landscapes. *Ecological Modelling* 135, 243–263. doi:10.1016/S0304-3800(00)00368-9.
- Himoto K, Iwami T (2021) Generalization framework for varying characteristics of the firebrand generation and transport from structural fire source. *Fire Safety Journal* 125, 103418. doi:10.1016/j.firesaf.2021.103418.
- Himoto K, Tanaka T (2005) Transport Of Disk-shaped Firebrands In A Turbulent Boundary Layer. *Fire Safety Science* 8, 433–444. doi:10.3801/IAFSS.FSS.8-433.

- Kaur I, Mentrelli A, Bosseur F, Filippi J-B, Pagnini G (2016) Turbulence and fire-spotting effects into wildland fire simulators. *Communications in Nonlinear Science and Numerical Simulation* 39, 300–320. doi:10.1016/j.cnsns.2016.03.003.
- Koo E, Pagni PJ, Weise DR, Woycheese JP (2010) Firebrands and spotting ignition in large-scale fires. *International Journal of Wildland Fire* 19, 818. doi:10.1071/WF07119.
- Manzello SL, Maranghides A, Mell WE (2007) Firebrand generation from burning vegetation. *International Journal of Wildland Fire* 16, 458. doi:10.1071/WF06079.
- Manzello SL, Shields JR, Cleary TG, Maranghides A, Mell WE, Yang JC, Hayashi Y, Nii D, Kurita T (2008) On the development and characterization of a firebrand generator. *Fire Safety Journal* 43, 258–268. doi:10.1016/j.firesaf.2007.10.001.
- Pérez Y, Pastor E, Àgueda A, Planas E (2011) Effect of Wind and Slope When Scaling the Forest Fires Rate of Spread of Laboratory Experiments. *Fire Technology* 47, 475–489. doi:10.1007/s10694-010-0168-7.
- Perryman HA, Dugaw CJ, Varner JM, Johnson DL (2013) A cellular automata model to link surface fires to firebrand lift-off and dispersal. *International Journal of Wildland Fire* 22, 428. doi:10.1071/WF11045.
- Sardoy N, Consalvi JL, Kaiss A, Fernandez-Pello AC, Porterie B (2008) Numerical study of ground-level distribution of firebrands generated by line fires. *Combustion and Flame* 154, 478–488. doi:10.1016/j.combustflame.2008.05.006.
- Sardoy N, Consalvi J, Porterie B, Fernandezpello A (2007) Modeling transport and combustion of firebrands from burning trees. *Combustion and Flame* 150, 151–169. doi:10.1016/j.combustflame.2007.04.008.
- Sofiev M, Ermakova T, Vankevich R (2012) Evaluation of the smoke-injection height from wild-land fires using remote-sensing data. *Atmospheric Chemistry and Physics* 12, 1995–2006. doi:10.5194/acp-12-1995-2012.
- Sullivan AL (2009a) Wildland surface fire spread modelling, 1990 - 2007. 1: Physical and quasi-physical models. *International Journal of Wildland Fire* 18, 349. doi:10.1071/WF06143.
- Sullivan AL (2009b) Wildland surface fire spread modelling, 1990 - 2007. 2: Empirical and quasi-empirical models. *International Journal of Wildland Fire* 18, 369. doi:10.1071/WF06142.
- Sullivan AL (2009c) Wildland surface fire spread modelling, 1990 - 2007. 3: Simulation and mathematical analogue models. *International Journal of Wildland Fire* 18, 387. doi:10.1071/WF06144.
- Sullivan AL, Cruz MG (2015) Small-scale flame dynamics provide limited insight into wildfire behavior. *Proceedings of the National Academy of Sciences* 112, E4164–E4164. doi:10.1073/pnas.1506877112.
- Suzuki S, Manzello SL, Lage M, Laing G (2012) Firebrand generation data obtained from a full-scale structure burn. *International Journal of Wildland Fire* 21, 961. doi:10.1071/WF11133.
- Tarifa CS, Marañón PP del NM de, Moreno FG, Villa AR (1967) Transport and Combustion of Firebrands. Final Report of Grants FG-SP-114 and FG-SP-146 Vol. II. INTA, Informe Técnico (Madrid) <http://oa.upm.es/6521/>.
- Tarifa CS, Notario PP del, Moreno FG (1965) On the flight paths and lifetimes of burning particles of wood. *Symposium (International) on Combustion* 10, 1021–1037. doi:10.1016/S0082-0784(65)80244-2.
- Thomas JC, Mueller EV, Santamaria S, Gallagher M, El Houssami M, Filkov A, Clark K, Skowronski N, Hadden RM, Mell W, Simeoni A (2017) Investigation of firebrand generation from an experimental fire: Development of a reliable data collection methodology. *Fire Safety Journal* 91, 864–871. doi:10.1016/j.firesaf.2017.04.002.
- Tihay V, Simeoni A, Santoni P-A, Rossi L, Garo J-P, Vantelon J-P (2009) Experimental study of laminar flames obtained by the homogenization of three forest fuels. *International Journal of Thermal Sciences* 48, 488–501. doi:10.1016/j.ijthermalsci.2008.03.018.
- Trucchia A, D'Andrea M, Baghino F, Fiorucci P, Ferraris L, Negro D, Gollini A, Severino M (2020) PROPAGATOR: An Operational Cellular-Automata Based Wildfire Simulator. *Fire* 3, 26. doi:10.3390/fire3030026.
- Trucchia A, Egorova V, Butenko A, Kaur I, Pagnini G (2019) RandomFront 2.3: a physical parameterisation of fire spotting for operational fire spread models – implementation in WRF-SFIRE and response analysis with LSFIRE+. *Geoscientific Model Development* 12, 69–87. doi:10.5194/gmd-12-69-2019.
- Wang H-H (2011) Analysis on Downwind Distribution of Firebrands Sourced from a Wildland Fire. *Fire Technology* 47, 321–340. doi:10.1007/s10694-009-0134-4.
- Wickramasinghe, A.; Khan, N.; Moinuddin, K. (2022) Determining Firebrand Generation Rate Using Physics-Based Modelling from Experimental Studies through Inverse Analysis. *Fire* 5, 6. doi: 10.3390/fire5010006

Werth PA, Potter BE, Clements CB, Finney MA, Goodrick SL, Alexander ME, Cruz MG, Forthofer JA, McAllister SS (2011) Synthesis of knowledge of extreme fire behavior: volume I for fire managers. U.S. Department of Agriculture, Forest Service, Pacific Northwest Research Station, PNW-GTR-854. (Portland, OR) doi:10.2737/PNW-GTR-854.